HE 1.3.3

INELASTIC CROSS-SECTIONS AND THEIR INFLUENCE ON AIR SHOWER DEVELOPMENT

J. Knapp[1*] for the KASCADE Collaboration[†]

[1] *Institut für Experimentelle Kernphysik, Universität Karlsruhe, D-76021 Karlsruhe, Germany*

ABSTRACT

In the extensive air shower simulation program CORSIKA the interaction models VENUS, QGSJET, SIBYLL, HDPM, and DPMJET are available to model high energy hadronic reactions. The inelastic cross-sections of nucleons, mesons and nuclei with nucleons and air nuclei as well as the particle production of the five models are examined and compared. The influence of the different models on air shower characteristics is presented.

INTRODUCTION

The interpretation of extensive air shower (EAS) measurements relies strongly on the model of the shower development in the Earth's atmosphere. The largest uncertainties originate from the hadronic interaction, which is not well known for high energies and small momentum transfers. Many models of hadronic interactions with a varying level of sophistication have been built, predominately around $p\bar{p}$ collider results using extrapolations to higher energies, to small angles and to nucleus-nucleus collisions. For comparison five hadronic interaction models widely used for EAS calculations were implemented in the CORSIKA air shower simulation program (Capdevielle et al., 1992, Knapp & Heck, 1993, Heck et al., 1997). These are HDPM, VENUS, QGSJET, SIBYLL, and DPMJET (for references see Heck et al., (1997)). In the following we present a comparison of the inelastic cross-sections adopted by the models and present results from shower calculations. For more details see Knapp et al. (1996).

INELASTIC CROSS-SECTIONS

All models deduce the hadron-air and nucleus-air cross-sections from the proton-antiproton cross-sections measured at the $p\bar{p}$ colliders and calculate from it the number of participating nucleons in projectile and target. Already the proton-proton cross-sections differ for the models. In Fig. 1a) the inelastic cross-sections of protons, pions, and kaons with protons are shown as a function of the laboratory momentum (symbols: collider results parameterized by the Particle Data Group). At low energies all models use comparable values for $\sigma^{\mathrm{pp}}_{\mathrm{inel}}$ or for $\sigma^{\pi\mathrm{p}}_{\mathrm{inel}}$. The differences are $< 10\%$. SIBYLL exhibits the flattest rise at low energies with values below the experimental results for 10^3 GeV/c $< p_{\mathrm{lab}} < 10^6$ GeV/c. At higher energies $\sigma^{\mathrm{pp}}_{\mathrm{inel}}$ of the SIBYLL model rises steeply and surpasses all other models. Similarly, $\sigma^{\pi\mathrm{p}}_{\mathrm{inel}}$ grows rapidly and reaches values of 100 mb at $p_{\mathrm{lab}} > 10^9$ GeV/c. Qualitatively such a behavior is expected. At low energies the ratio $\sigma^{\pi\mathrm{p}}/\sigma^{\mathrm{pp}}$ should roughly represent the ratio of the number of valence quarks, i.e. 2/3. With rising energy gluon-gluon reactions become dominant and consequently pion and nucleon cross-sections approach each other and their ratio rises towards unity. This behavior is obvious for SIBYLL and, less pronounced, for QGSJET. The cross-sections of QGSJET also rise with energy, but agree better with experimental data at low energies. The pronounced rise for these models is due to minijet production. The cross-sections of VENUS exhibit the slowest rise with energy due to the absence of hard processes, which increasingly contribute to the cross-sections with rising energy. The ratio of p, π, and K cross-sections are assumed

*corresponding author: e-mail: knapp@ik1.fzk.de

†The full list of authors and institutions of the KASCADE Collaboration is given at the end of this volume.

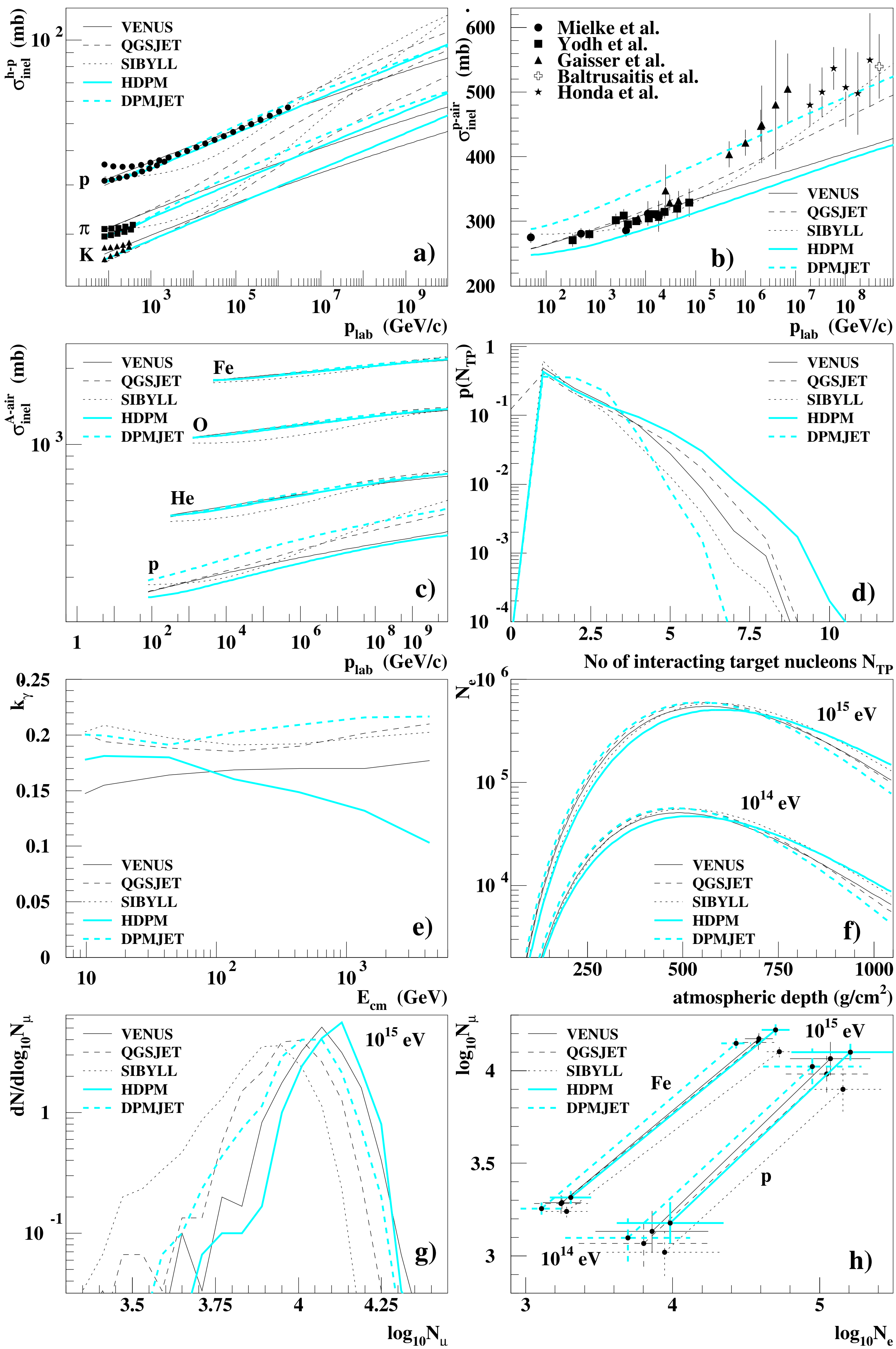

Fig. 1: Cross-sections, particle distributions, and shower development for different hadronic interaction models. (For explanations see text.)

to be constant in VENUS and HDPM. The models differ by more than 100% for high energy pions and by about 50% for protons. SIBYLL and DPMJET adopt the pion cross-sections as well for kaons, whereas in the other models the kaon cross-sections are 30% below the pion cross-sections. In Fig. 1b) the inelastic cross-sections for collisions of protons with air are shown together with experimental results from air shower analyses and from single hadron measurements (Mielke et al., 1994; Gaisser et al., 1987; Yodh et al., 1983; Honda et al., 1993; Baltrusaitis et al., 1993). The cross-sections behave qualitatively similar to the ones in Fig. 1a) but the differences between the models are larger. SIBYLL cross-sections exhibit a flat part at low energies and the steepest rise at high energies. This does not reproduce the collider cross-sections but describes the air shower data best. SIBYLL fits well $\sigma_{\rm inel}^{\rm p-air}$ at $p \approx 50$ GeV/c of Mielke et al., (1994) and of the Particle Data Group of $\sigma_{\rm inel}^{\rm p-air} \approx 270$ mb. The other models differ by up to 25 mb (10%) from this value. Using $\sigma_{\rm inel}^{\rm pp}$ and the Glauber theory generally a much flatter rise of $\sigma_{\rm inel}^{\rm p-air}$ is predicted than air shower experiments indicate at high energies. However, a recent reanalysis of single hadron and AKENO data by Bellandi et al. (1997) claims cross-sections at $E > 10^7$ GeV which are only 70% of the values shown in Fig. 1b) and, thus, agree even with the flat extrapolation of HDPM. Models which show comparable energy dependencies in Fig. 1a), differ in Fig. 1b) by 50 to 75 mb or 25 to 40%, respectively[1]. This reflects the different ways of calculating $\sigma_{\rm inel}^{\rm p-air}$ from $\sigma_{\rm inel}^{\rm pp}$, e.g. different assumptions on the shape of the target nuclei. In Fig. 1c) the inelastic nucleus-air cross-sections are shown as used in CORSIKA. SIBYLL provides its own nucleus-air cross-section table, while for the other models we take the model specific proton-proton cross-sections and use the CORSIKA Glauber probabilities to derive nucleus-nucleus cross-sections. For DPMJET and VENUS it is possible to calculate their own nucleus-nucleus cross-sections in a time consuming manner. They differ from the cross-sections shown by $< 8\%$. With rising projectile mass the differences decrease. The SIBYLL cross-sections are slightly below the other models with a form similar to $\sigma_{\rm inel}^{\rm pp}$.

PARTICLE PRODUCTION

The assumed shape of a nucleus not only influences $\sigma_{\rm inel}$ but determines also the number of participating nucleons and, therefore, the energy available for secondary particle production. Fig. 1d) shows the distributions of the number of target participants in p-^{14}N collisions. All models except HDPM adopt the charge distribution of a nucleus for its nucleon distribution. HDPM correctly deconvolves the known charge distribution of the proton leading to smaller and denser nuclei and, consequently, to more participants on average. The fraction of the incident energy carried away by electromagnetic particles $k_\gamma = \sum E_\gamma/E_0$ influences strongly the EAS development. In Fig. 1e) $\langle k_\gamma \rangle$ in p-^{14}N collisions is shown depending on the cm energy. Except for HDPM the models show nearly energy independent k_γ, the spread between the models is of the order of 25%. Since diffractive events have small k_γ the cross-sections for diffractive events are relevant, too.

AIR SHOWER CALCULATIONS

To investigate the shower development vertical proton and iron induced showers of 10^{14} and 10^{15} eV have been simulated with CORSIKA using the 5 hadronic interaction models for $E_{\rm lab} > 80$ GeV/n. The average particle numbers for several secondaries in 10^{15} eV showers are listed in Table 1. Variations of both, $\sigma_{\rm inel}$ and k_γ, induce primarily a shortening or elongation of the shower. The precise form of the longitudinal distribution depends on a combination of both quantities. It is shown for 10^{14} and 10^{15} eV proton showers in Fig. 1f). Large cross-sections combined with a high inelasticity (DPMJET e.g.) lead to short showers with a small electron number at ground level whereas small inelasticity and cross-sections give long showers and

---

[1] The cross-section $\sigma_{\rm inel}^{\rm p-air}$ for DPMJET is too high due to a fault in the DPMJET version available for this comparison. In the next version of DPMJET it will be corrected.

Table 1: Average particle numbers and variances for 10^{15} eV p and Fe showers at 110 m a.s.l..

10^{15} eV Protons					
	VENUS	QGSJET	SIBYLL	HDPM	DPMJET
p	589.6 ± 270.9	360.4 ± 186.5	428.4 ± 200.6	578.9 ± 230.1	512.5 ± 251.8
$\overline{p}$	19.9 ± 12.6	9.4 ± 7.3	10.5 ± 7.2	20.0 ± 11.8	13.4 ± 11.0
n	1265.9 ± 495.9	797.5 ± 348.4	888.3 ± 368.7	1206.5 ± 402.0	1134.8 ± 463.5
$\overline{n}$	25.4 ± 15.4	11.9 ± 8.9	13.0 ± 8.3	23.7 ± 13.3	17.6 ± 12.3
$\mu^{\pm}$	11618 ± 2475	9577 ± 2266	7921 ± 2210	12591 ± 2314	10546 ± 2466
$\pi^{\pm}$	213.9 ± 178.8	157.1 ± 149.5	200.7 ± 152.3	263.6 ± 250.7	128.2 ± 125.6
K_L^0	5.4 ± 5.6	4.1 ± 4.4	4.2 ± 4.2	5.9 ± 5.1	2.7 ± 3.5
$K^{\pm}$	4.2 ± 5.3	2.9 ± 4.2	3.4 ± 4.2	5.3 ± 5.5	2.0 ± 3.4
$e^{\pm}$	118301 ± 79991	112097 ± 88139	144704 ± 86254	162209 ± 91309	89184 ± 66176
10^{15} eV Iron					
	VENUS	QGSJET	SIBYLL	HDPM	DPMJET
p	478.4 ± 77.9	348.6 ± 69.0	434.1 ± 70.1	457.5 ± 78.9	422.8 ± 69.3
$\overline{p}$	11.5 ± 4.3	6.4 ± 2.9	7.7 ± 3.2	11.3 ± 4.5	7.6 ± 3.3
n	1131.1 ± 155.7	837.4 ± 145.1	999.3 ±132.3	1063.1 ±155.4	1044.4 ± 143.0
$\overline{n}$	15.6 ± 4.9	8.8 ± 3.6	9.6 ± 3.7	13.7 ± 4.6	10.3 ± 3.9
$\mu^{\pm}$	14897 ± 1028	14216 ± 1388	12664 ± 798	16644 ±1135	14053 ± 937
$\pi^{\pm}$	107.0 ± 36.3	93.3 ± 35.4	117.9 ± 37.4	168.3 ± 55.2	61.7 ± 24.1
K_L^0	2.3 ± 1.9	2.0 ± 1.7	2.1 ± 1.6	2.3 ± 1.7	1.0 ± 1.1
$K^{\pm}$	1.5 ± 2.0	1.1 ± 1.7	1.5 ± 1.8	1.9 ± 2.2	0.7 ± 1.3
$e^{\pm}$	38724 ± 8267	38324 ± 9658	53234 ± 11146	50370 ± 11081	27103 ± 6230

$E_{e^{\pm}} > 3$ MeV, $E_{\mu}, E_h > 100$ MeV

large N_e (HDPM e.g.). N_e at ground level differs by a factor of 2 entailing a similar systematic uncertainty when deducing the primary energy from N_e only. Iron showers have about 60% smaller N_e and 25% larger N_μ than proton showers. The muon numbers predicted by VENUS, QGSJET, and DPMJET agree within 20%, while SIBYLL predicts about 60% smaller values for proton showers. The N_μ distribution of SIBYLL (Fig. 1g)) shows for proton showers a pronounced tail to small N_μ. This tail is of relevance when identifying photon induced showers by their small number of muons. The average values of N_e and N_μ for different primaries and energies are shown in the $\log N_e$-$\log N_\mu$ plane in Fig. 1h). The differences between proton and iron showers remain larger than the differences between the models.

CONCLUSIONS

Using different hadronic interaction models in air shower calculations leads to markedly different prediction of typical air shower observables. The electron numbers at ground level vary for proton showers by up to a factor of 2, the muon numbers by up to 60%. Consequently, the systematic uncertainties in air shower analyses amount up to 100%. The differences between the models are so large that precise experiments should be able to discriminate between them.

REFERENCES

Baltrusaitis, R.M. et al., *Phys. Rev. Lett.*, **52**, 1380 (1993).
Bellandi, J. et al., *J. Phys. G: Nucl. Part. Phys.*, **23**, 125 (1997).
Capdevielle, J.N. et al., *Kernforschungszentrum Karlsruhe*, **KfK 4998** (1992).
Gaisser, T.K. et al., *Phys. Rev. D*, **36**, 1350 (1987).
Heck, D., Knapp, J., *Proc. 25th Int. Cosmic Ray Conference, Durban*, **HE 2.3.2** (1997).
Honda, M. et al., *Phys. Rev. Lett.*, **70**, 525 (1993).
Knapp, J., Heck D., *Kernforschungszentrum Karlsruhe*, **KfK 5196 B** (1993).
Knapp, J. et al., *Forschungszentrum Karlsruhe*, **FZKA 5828** (1996).
Mielke, H.H. et al., *J. Phys. G: Nucl. Part. Phys.*, **20**, 637 (1994).
Yodh, G.B. et al., *Phys. Rev. D*, **27**, 1183 (1983).